HNPS Advances in Nuclear Physics

Vol 32 (2026)

HNPS2025

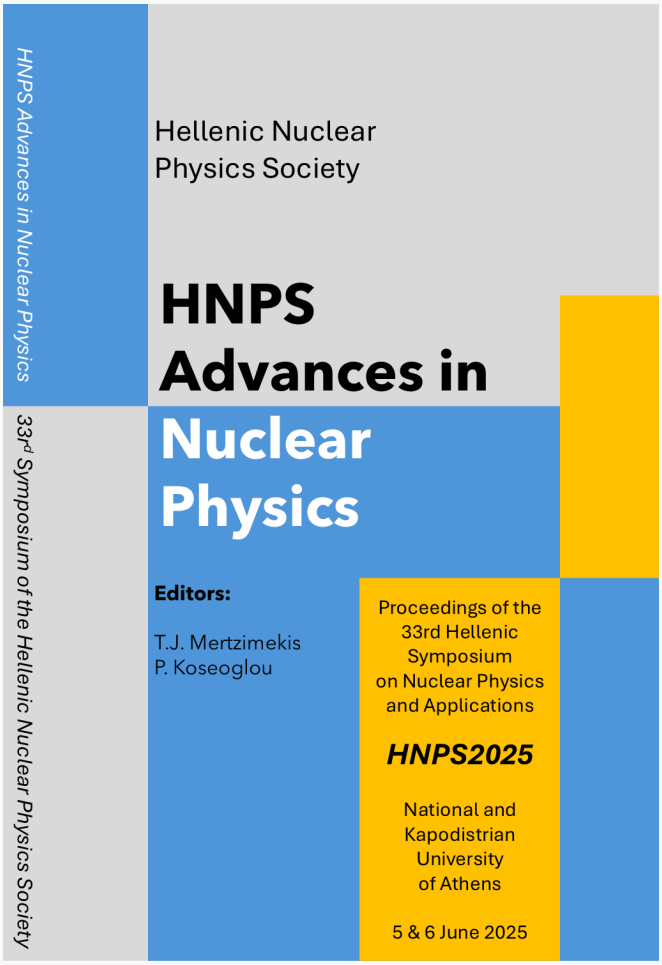

Reaction mechanism for 8B+ natZr at the sub-Coulomb energy of 26.5 MeV

Konstantina Palli, Athina Pakou, Antonio Moro, Patrick O'Malley, Luis Acosta, Angel Sánchez-Bénitez, George Souliotis, Eli Aguilera, Eduardo Andrade, David Godos, Onoufrios Sgouros, Vasileios Soukeras, Clementina Agodi, Thomas Bailey, Dan Bardayan, Chevelle Boomershine, Maxime Brodeur, Francesco Cappuzello, Scott Caramichael, Manuela Cavallaro, Stefania Dede, Jose Duenas, Joseph Henning, Kevin Lee, William Porter, Fabio Rivero, William von Seeger

doi: 10.12681/hnpsanp.8668

Godos, D., Sgouros, O., Soukeras, V., Agodi, C., Bailey, T., Bardayan, D., Boomershine, C., Brodeur, M., Cappuzello, F., Caramichael, S., Cavallaro, M., Dede, S., Duenas, J., Henning, J., Lee, K., Porter, W., Rivero, F., & von Seeger, W. (2026). Reaction mechanism for 8B+ natZr at the sub-Coulomb energy of 26.5 MeV. *HNPS Advances in Nuclear Physics*, *32*, 158–163. https://doi.org/10.12681/hnpsanp.8668

HNPS Advances in Nuclear Physics Vol. **32**, 158–163 (2025)
doi: 10.12681/hnpsanp.8668

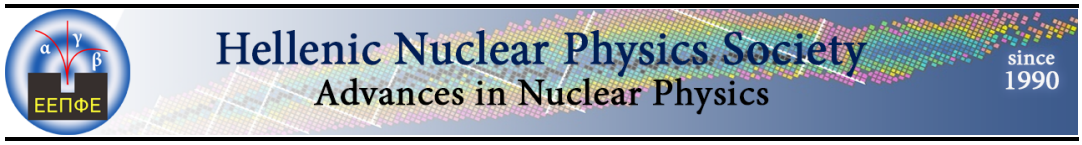

ARTICLE

Reaction mechanism for ^{8}B+^{nat}Zr at the sub-Coulomb energy of 26.5 MeV

K. Palli,[*,1,2] A. Pakou,[1] A. M. Moro,[3,4] P. D. O'Malley,[5] L. Acosta,[6] A. Sánchez-Bénitez,[7] G. Souliotis,[2] E. F. Aguilera,[8] E. Andrade,[6] D. Godos,[6] O. Sgouros,[9,10] V. Soukeras,[9,10] C. Agodi,[9] T. L. Bailey,[5] D. W. Bardayan,[5] C. Boomershine,[5] M. Brodeur,[5] F. Cappuzzello,[9,11] S. Caramichael,[5] M. Cavallaro,[9] S. Dede,[5,12] J. A. Dueñas,[13] J. Henning,[5] K. Lee,[5] W. S. Porter,[5] F. Rivero,[5] and W. von Seeger[5]

[1]Department of Physics, The University of Ioannina, 45110 Ioannina, Greece
[2]Department of Chemistry, National and Kapodistrian University of Athens, 15771 Athens, Greece
[3]Departamento de Física Atómica, Molecular y Nuclear, Universidad de Sevilla, Apartado 1065, E-41080 Sevilla, Spain
[4]Instituto Interuniversitario Carlos I de Física Teórica y Computational (iC1), Apartado. 1065, E-41080 Sevilla, Spain
[5]Department of Physics and Astronomy, University of Notre Dame, Notre Dame, Indiana 46556, USA
[6]Instituto de Física, Universidad Nacional Autónoma de México, A.P. 20-364, México City 01000, México
[7]Departamento de Ciencias Integradas y Centro de Estudios Avanzados en Física, Matemáticas y Computatión, Universidad de Huelva, 21071 Huelva, Spain
[8]Departamento de Aceleradores y Estudio de Materiales, Instituto Nacional de Investigaciones Nucleares, Apartado Postal 18-1027, Codigo Postal 11801, Mexico City, Distrito Federal, Mexico
[9]INFN Laboratori Nazionali del Sud, via Santa Sofia 62, 95125 Catania, Italy
[10]Dipartimento di Fisica e Astronomia "Ettore Majorana", Universita di Catania, via Santa Sofia 64, 95125 Catania, Italy
[11]Dipartimento di Fisica e Astronomia "Ettore Majoran"", Universita di Catania, via Santa Sofia 64, 95125 Catania, Italy
[12]Cyclotron Institute, Texas A&M University, College Station, Texas 77843, USA
[13]Centro de Estudios Avanzados en Física, Matemáticas y Computatión, Universidad de Huelva, 21071 Huelva,Spain

*Corresponding author: konstpalli@gmail.com

(Received: 25 Sep 2025; Accepted: 13 Jan 2026; Published: 28 Jan 2026)

Abstract

We will present a survey of our recent results on the reaction mechanism of ^{8}B+^{nat}Zr below the Coulomb barrier. Elastic scattering and breakup measurements were previously performed at 26.5 MeV (90% of the Coulomb barrier) at the TriSol radioactive ion beam facility of the University of Notre Dame. Complementary elastic scattering results were also obtained for the core of ^{8}B, the ^{7}Be nucleus, at various sub- and near-barrier energies. Total reaction and breakup cross sections, as well as critical interaction distances, were determined and compared with existing results for weakly and well-bound projectiles on various targets. The results indicate the importance of direct mechanisms below barrier and the distinction between weakly-bound and well-bound projectiles.

Keywords: exotic nuclei, total reaction cross section, elastic scattering, breakup

 ISBN 2654-007X (print), 2654-0088 (online).

1. Introduction

The study of weakly-bound and exotic nuclei has attracted considerable attention due to their unusual structures and low breakup thresholds. At low energies, their Optical Potential differs from that of stable nuclei, strongly affecting the reaction mechanism, where direct processes such as transfer and breakup dominate over fusion, with significant effects in astrophysics [1–4]. For weakly-bound nuclei, phenomenological predictions reported in [4] show that the direct-to-total reaction cross section ratio remains constant ~0.2 above the barrier, but rises sharply with decreasing energy, saturating at 0.7 for light, 0.8 for medium-mass, and 1.0 for heavy targets, further indicating a direct-channel dominance. The exotic nucleus ^{8}B is an ideal candidate to investigate breakup dominance over fusion. Its halo structure [5–7] and very low breakup threshold of 137 keV suggest large breakup cross sections, though its proton halo could reinforce the barrier and reduce breakup probability. Motivated by this and following our previous ^{8}B+^{208}Pb study [8], we have previously performed elastic scattering and breakup measurements for ^{8}B on a medium-mass ^{nat}Zr target at the sub-barrier energy of 26.5 MeV [9, 10], as well as elastic scattering measurements of its core nucleus ^{7}Be+^{nat}Zr at various sub- and near-barrier energies [11]. A short survey of this work will be presented in this article, referring to the phenomenological analysis of our cross section and critical interaction distances results and their extensive comparison with various other systems. The general aim was to probe the reaction mechanisms at sub- and near- barrier energies.

2. Experimental Results

Elastic scattering and breakup measurements for ^{8}B+^{nat}Zr were performed at the TriSol radioactive ion beam facility [12], along with elastic scattering for ^{7}Be+^{nat}Zr [11] under the same experimental conditions. Experimental details are reported in [9–11].

Total reaction cross sections

From the phenomenological analysis of the elastic scattering angular distributions for both ^{7}Be and ^{8}B [9, 11] on the ^{nat}Zr target, total reaction cross sections were extracted and are presented in Table 1. The total reaction cross sections of Table 1 along with total reaction cross sections for various projectiles and targets were reduced by using the formulas reported in [13] to remove barrier effects, and are presented in Fig. 1. It should be noted that the black solid line is a fit to data for exotic projectiles, and the red dashed line fits data for weakly- and well-bound projectiles. Reduced cross sections are enhanced for exotic nuclei below the Coulomb barrier, with convergence at higher energies. Target dependence is also apparent. For clarity, the right panel shows only medium-mass targets, highlighting the enhancement for ^{8}B, shown with the black circle. At 90% of the barrier, its reduced cross section is ~12 times larger than its core, ^{7}Be, providing strong evidence of the proton-halo effect.

Table 1. Total reaction cross sections for ^{8}B, ^{7}Be + ^{nat}Zr.

System	E_{lab} (MeV)	σ_{tot} (mb)
^{8}B + ^{nat}Zr	26.5	180 ± 40
^{7}Be + ^{nat}Zr	19.7	6 ± 4
	21.3	45 ± 11
	22.9	260 ± 20
	26.6	545 ± 30
	27.5	638 ± 60

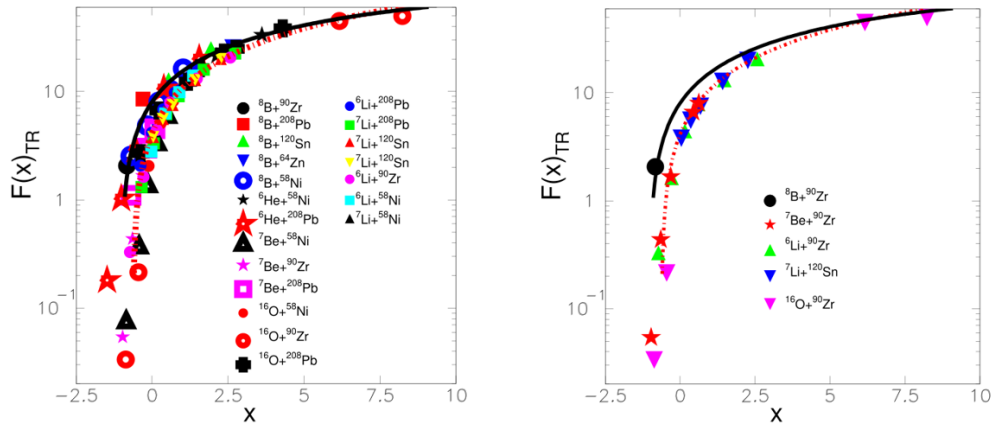

Figure 1. Left panel: Reduced total reaction cross sections over reduced energy [14] for various systems, the black line is a fit to the data for exotic projectiles and the dashed red line a fit to data for well- and weakly-bound projectiles. Right panel: Same as in the left panel, only for medium-mass targets. Data from [9] and references therein.

Critical interaction distance

The reduced critical interaction distances for the present and other systems, calculated according to [15], are plotted against the product of projectile and target atomic numbers, Z_1Z_2, in Fig. 2. This distance marks the beginning of nuclear effects, where elastic scattering deviates from the Rutherford scattering predictions. It is defined as the distance of closest approach at the angle where the elastic-to-Rutherford ratio is ~0.98 [15–18] and the extraction of this value for the different systems is described in [9]. Fig. 2 reveals the existence of three distinct groups.

The first group, indicated by black points and black dashed line, corresponds to exotic nuclei: ^{8}B, ^{6}He, and ^{8}Li. It should be noted that for this group, the critical interaction distances follow an almost constant trend, suggesting that for nuclei with extended nuclear matter, the nuclear interaction begins at similarly large distances. This behavior further supports the possible presence of a neutron skin in ^{8}Li.

On the other hand, the weakly-bound nuclei ^{7}Be, ^{6}Li, and ^{7}Li+^{58}Ni are described by a separate curve, marked by the blue dotted-dashed line, in Fig. 2. This behavior differs from that of well-bound nuclei, represented by the red dotted line, which includes ^{16}O and the weakly-bound stable ^{7}Li on the heavy targets ^{120}Sn and ^{208}Pb. Notably, the weakly- and well-bound groups cross at the reduced distance of ^{16}O+^{208}Pb. This may indicate that for systems with large product Z_1Z_2, the nuclear interaction begins only at very small distances both for weakly- and well-bound nuclei.

Breakup cross sections

The CDCC analysis of the breakup angular distributions for ^{8}B+^{nat}Zr lead to a breakup cross section of σ = 170 ± 40 mb [10] which combined with the total reaction cross section, results in a direct-to-total reaction cross section ratio of r = 0.95 ± 0.23. This high value shows that breakup nearly exhausts the total reaction cross section, revealing the dominance of the breakup channel. The current result, shown in Fig. 3 (green star), is compared with other weakly-bound nuclei and predictions from [4]. For ^{8}B on ^{nat}Zr, the ratio is larger than the expected value of 0.8 for medium-mass targets. However, the large uncertainty prevents from drawing firm conclusions.

Furthermore we have compared breakup cross sections for ^{8}B on various targets. The reduction

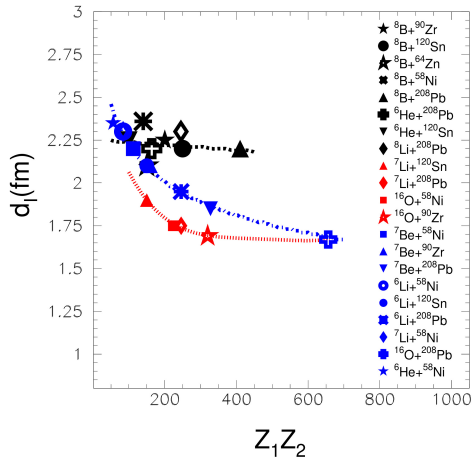

Figure 2. Critical interaction distances over $Z_p Z_t$ for various projectiles and targets. Black line and points correspond to exotic nuclei: ^{8}B, ^{6}He and ^{8}Li, blue line and points correspond to weakly-bound nuclei ^{7}Be, ^{6}Li and ^{7}Li+^{58}Ni and red line and points correspond to the well-bound nucleus ^{16}O and the weakly-bound nucleus ^{7}Li on heavy targets. Data from [9] and references therein.

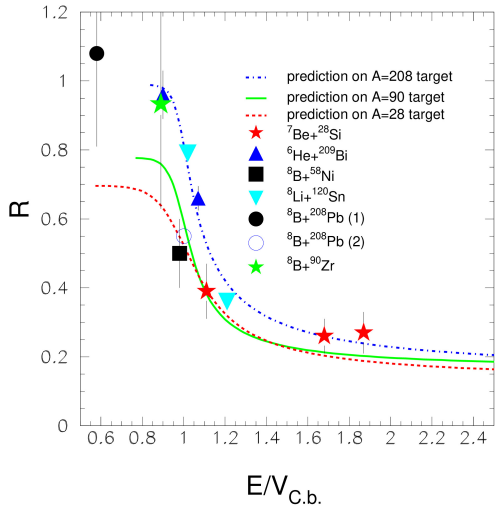

Figure 3. Direct-to-total reaction cross section ratio versus the energy over Coulomb barrier. The lines correspond to phenomenological predictions reported in [4] for light (red), medium-mass (green) and heavy (blue) targets. Figure from [10].

of the breakup cross sections were performed with two methods following the prescriptions from Ref. [14] (Fig. 4a) and Ref. [19] (Fig. 4b). Fig. 4c shows the comparison of the breakup cross sections over the distance of closest approach for a head-on collision. In all three plots of Fig. 4 we can observe a strong target dependence with a clear differentiation between systems with medium-mass and heavy targets.

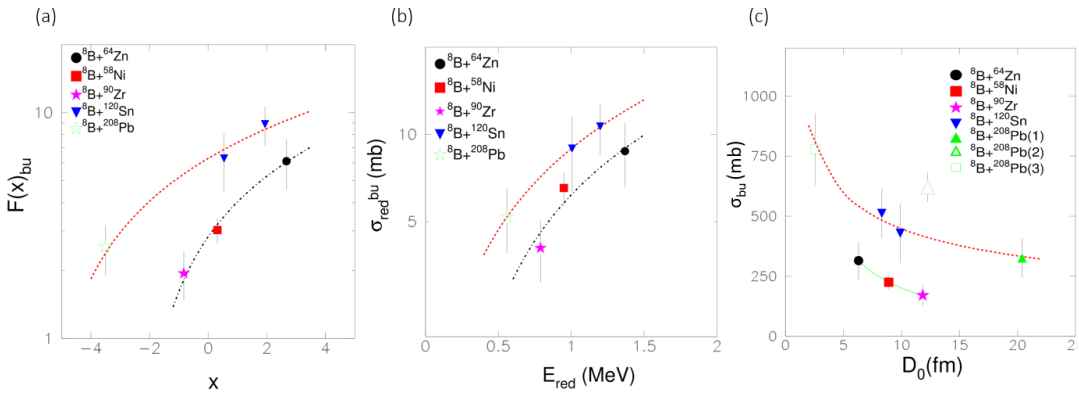

Figure 4. Comparison of breakup cross sections for ^{8}B on various targets. (a) Reduced breakup cross sections over reduced energy, according to [14]. (b) Reduced breakup cross sections over reduced energy, according to [19]. (c) Breakup cross sections over distance of closest approach for a head-on collision. Data from [10] and references therein.

3. Summary and Conclusions

We have summarized our experimental results of elastic scattering and breakup measurements for the reaction ^{8}B+^{nat}Zr at 26.5 MeV (~90% of the Coulomb barrier) and the elastic scattering of the ^{8}B core, ^{7}Be, on the same target. Total reaction and breakup cross sections were determined and compared with existing data for various systems. The main conclusions are:

- Breakup is the dominant reaction mechanism for ^{8}B at energies below the barrier.
- The direct-to-total reaction cross section ratio, at $E/V_{C.b.} \approx 0.9$ was determined as ~0.95 ± 0.23, a value larger than the expected one for a medium-mass target, ~0.8.
- Reduced total reaction cross sections show an enhancement for exotic nuclei below the barrier, while convergence occurs at higher energies. At ~90% of the barrier, the reduced cross section of ^{8}B is approximately 12 times larger than the one of its core ^{7}Be, indicating proton halo.
- Critical interaction distances plotted against Z_1Z_2 reveal three distinct groups of exotic, weakly bound, and well-bound nuclei, each following a different trend. The main conclusion here is that reactions for all exotic nuclei start at larger distances as the projectile approaches the target, with a consequence of higher cross sections than standard. For other weakly-bound nuclei this distance is smaller but still larger than that of well-bound nuclei with a clear dependence on the product Z_1Z_2. For very large values of the product Z_1Z_2, the critical interaction distance is similar for both weakly-bound, but stable, and well-bound nuclei. For all three groups there is a convergence at very small Z_1Z_2.
- The halo nuclei ^{8}B and ^{6}He display similar behavior, while ^{8}Li follows the exotic-nuclei trend as well, supporting evidence for a neutron skin.
- Breakup cross sections versus distance of closest approach and reduced cross sections versus reduced energy show a clear target dependence, with medium-mass and heavy targets following distinct trends, with the former exhibiting lower cross sections.

Acknowledgments

K.P. acknowledges support by the Hellenic Foundation for Research and Innovation (HFRI) under the 4th Call for HFRI PhD Fellowships, No. 009194. We acknowledge support from the National

Science Foundation Grant No. PHY-2310059.

References

[1] L. F. Canto et al. "Fusion and breakup of weakly bound nuclei". In: *Phys. Rep.* 424 (2006), p. 1. DOI: 10.1016/j.physrep.2005.10.006.

[2] N. Keeley et al. "Fusion and direct reactions of halo nuclei at energies around the Coulomb barrier". In: *Prog. Part. Nucl. Phys.* 59 (2007), p. 579. DOI: 10.1016/j.ppnp.2007.02.002.

[3] A. Pakou et al. "Reaction mechanisms of the weakly bound nuclei ^{6,7}Li and ^{7,9}Be on light targets at near barrier energies". In: *Eur. Phys. J. A* 58 (2022), p. 8. DOI: 10.1140/epja/s10050-021-00655-w.

[4] A. Pakou et al. "Important influence of single neutron stripping coupling on near-barrier ^{8}Li + ^{90}Zr quasi-elastic scattering". In: *Eur. Phys. J. A* 51 (2015), p. 55. DOI: 10.1140/epja/i2015-15090-3.

[5] I. Tanihata et al. "Measurement of interaction cross sections using isotope beams of Be and B and isospin dependence of the nuclear radii". In: *Phys. Lett. B* 206 (1987), p. 4. DOI: 10.1016/0370-2693(88)90702-2.

[6] T. Minamisono et al. "Proton halo of ^{8}B disclosed by its giant quadrupole moment". In: *Phys. Rev. Lett.* 69 (1992), p. 2058. DOI: 10.1103/PhysRevLett.69.2058.

[7] E. F. Aguilera et al. "Reaction cross sections for ^{8}B, ^{7}Be, and ^{6}Li +^{58}Ni near the Coulomb barrier: Proton-halo effects". In: *Phys. Rev. C* 79 (2009), p. 021601. DOI: 10.1103/PhysRevC.79.021601.

[8] A. Pakou et al. "Dominance of direct reaction channels at deep sub-barrier energies for weakly bound nuclei on heavy targets: The case ^{8}B+^{208}Pb". In: *Phys. Rev. C* 102 (2020), p. 031601. DOI: 10.1103/PhysRevC.102.031601.

[9] K. Palli et al. "Elastic scattering of ^{8}B+^{nat}Zr at the sub-barrier energy of 26.5 MeV". In: *Phys. Rev. C* 109 (2024), p. 064614. DOI: 10.1103/PhysRevC.109.064614.

[10] K. Palli et al. "Breakup of the proton halo nucleus ^{8}B at a sub-Coulomb energy". In: *Phys. Rev. C* 111 (2025), p. 024615. DOI: 10.1103/PhysRevC.111.024615.

[11] K. Palli et al. "Quasielastic scattering of ^{7}Be+^{nat}Zr at sub- and near-barrier energies". In: *Phys. Rev. C* 107 (2023), p. 064613. DOI: 10.1103/PhysRevC.107.064613.

[12] P. D. O'Malley et al. "TriSol: A major upgrade of the TwinSol RNB facility". In: *Nucl. Instrum. Meth. A* 1047 (2023), p. 167784. DOI: 10.1016/j.nima.2022.167784.

[13] V. Guimarães et al. "Nuclear and Coulomb Interaction in ^{8}B Breakup at Sub-Coulomb Energies". In: *Phys. Rev. Lett.* 84 (2000), p. 1862. DOI: 10.1103/PhysRevLett.84.1862.

[14] L. F. Canto et al. "Disentangling static and dynamic effects of low breakup threshold in fusion reactions". In: *J. Phys. G: Nucl. Part. Phys.* 36 (2009), p. 015109. DOI: 10.1088/0954-3899/36/1/015109.

[15] A. Pakou and K. Rusek. "Interaction distances for weakly bound nuclei at near barrier energies". In: *Phys. Rev. C* 69 (2004), p. 057602. DOI: 10.1103/PhysRevC.69.057602.

[16] B. T. Kim et al. "Semiclassical character and optical model description of heavy ion scattering, direct reactions, and fusion at near-barrier energies". In: *Phys. Rev. C* 65 (2002), p. 044607. DOI: 10.1103/PhysRevC.65.044607.

[17] P. R. Christensen et al. "A study of ^{16,18}O and ^{12}C induced reactions on A = 40–96 nuclei". In: *Nucl. Phys. A* 207 (1973), pp. 33–77. DOI: 10.1016/0375-9474(73)90023-7.

[18] V. Guimarães et al. "Phenomenological critical interaction distance from elastic scattering measurements on a ^{208}Pb target". In: *Eur. Phys. J. A* 54 (2018), p. 223. DOI: 10.1140/epja/i2018-12662-7.

[19] P. R. S. Gomes et al. "Uncertainties in the comparison of fusion and reaction cross sections of different systems involving weakly bound nuclei". In: *Phys. Rev. C* 71 (2005), p. 017601. DOI: 10.1103/PhysRevC.71.017601.